

Selectivity of lipases: Conformational analysis of suggested intermediates in ester hydrolysis of chiral primary and secondary alcohols

J. Zuegg^{a,*}, H. Hönig^a, J.D. Schrag^b, M. Cygler^b

^a Institute for Organic Chemistry and SFB Biokatalyse, Technical University Graz, Stremayrgasse 16, A-8010 Graz, Austria

^b Biotechnology Research Institute, 6100 Royalmount Avenue, Montréal, Que., Canada H4P 2R2

Abstract

Conformational analysis of the proposed tetrahedral transition state of different *model esters* in the active sites of the lipases of *Candida rugosa* and *Pseudomonas cepacia* are used to analyze structural reasons for the unique enantiomeric preference of lipases towards the cleavage of esters of chiral primary and secondary alcohols. The results are compared with the existing rules for the preference of one specific enantiomer in the hydrolysis of esters of chiral alcohols. Interesting results on the dynamics behaviour of some enantiomers within the lipases are reported.

Keywords: Lipase; *Candida rugosa*; *Pseudomonas cepacia*; Crystal structure comparison; Enantioselectivity model; Molecular mechanics; Molecular dynamics; Monte-Carlo minimization; Substrate orientations; Ester residue alignments

1. Introduction

Lipases and esterases are enzymes hydrolyzing a variety of different esters. Although the original function of lipases is to hydrolyze triglycerides into glycerol and fatty acids [1], they are widely used in the synthesis of organic compounds for the preparation of chiral intermediates [2]. The enantiomeric differentiation of lipases is used to separate racemic mixtures of chiral esters by hydrolyzing preferentially one enantiomer of the ester or in esterification reactions of chiral acids and/or chiral alcohols. Mapping of the specificity of different lipases revealed unique tendencies, which led to simple

rules to predict which enantiomer reacts faster. These rules are either based on the size of the substituents at the stereocenter of the substrate by defining favored orientations of large and medium sized substituents, or by defining boxes for the supposed binding site and then trying to fit in the respective substrates. In that way, rules for the selectivities of hydrolases towards secondary alcohol esters [3–7] and chiral primary alcohol esters [7–9] have been developed for several lipases and esterases. While the rules for secondary alcohols are consistent, the models for primary alcohols are not that convincing. Even by including into the rules binding properties by defining hydrophobic and polar pockets [10–12] no satisfactory general principle for most of the observed experimental results was found. For chiral primary alcohols there are for

* Corresponding author.

e.g. different rules with or without oxygen at the asymmetric center, respectively, reflecting the ambiguous nature of those rules. For the selectivity of hydrolases towards chiral acids only rules for pig liver esterase [13–16] and *Candida rugosa* lipase [17,18] are developed by now.

Common to those empirical rules is the fact that they are based on the mapping of many different chemical structures of esters hydrolyzed by the enzymes. Recent determinations of crystal structures of several lipases now open the possibility to extend and unify these rules by structural information of the active sites.

The reaction mechanism catalyzed by lipases is assumed to be analogous to that of serine proteases [19]. This mechanism involves the formation of two tetrahedral intermediates, where the first (TI₁) is leading to an acyl enzyme and the second (TI₂) leads either to the acid (with water) or to the transesterificated ester [20] (see Fig. 1). Therefore, the first tetrahedral intermediate TI₁ determines the selectivity of the lipase towards alcohols because the alcohol leaves the acyl enzyme at this step. The selectivity towards carboxylic acids is determined by both tetrahedral intermediates as both contain the carboxylic acid moiety. The intermediate itself is formed by a hydrogen transfer from the serine to the imidazole ring of the histidine residue thus forming a positively charged imidazole ring [21] which is stabilized by the nearby aspartate and glutamate residues.

In addition to a common sequence pattern

around the active site serine (Gly–X–Ser–X–Gly), the known three-dimensional structures of the lipases show a unique framework in their tertiary structures. This conserved fold, called α/β hydrolase fold [22,23], is believed to impose a common stereoselectivity pattern for the catalytic activity of the entire superfamily [24]. Strictly, this can be applied only to the attack of the serine oxygen at the carbon atom of the carbonyl group [25] and thus to the orientation of the whole substrate (ester) with respect to the catalytic triad. This is also reflected in our modeling of triglycerides within *Candida rugosa* lipase [26], which gave a unique orientation of the carbonyl group. But this fact does not reflect the preferred orientation of the alcohol part of the ester within the active site, because the asymmetric center of the alcohol is too far away from the serine residue. Thus we believe that other steric and/or electronic features are responsible for the enantioselectivity of lipases within the reactions mentioned above.

Many lipases have a flexible loop (lid) which can cover the active site. Brownian-dynamic simulations on a triose phosphate isomerase with glyceraldehyde 3-phosphate as substrate [27] show no influence of the flexible loop on the access of substrates because the lid's opening and closing is faster than the diffusion of substrates into the active site [28]. Thus the loop could close while the substrate is in the binding site. On the other hand, cutinase from *Fusarium solani*, which has no lid, shows the same enan-

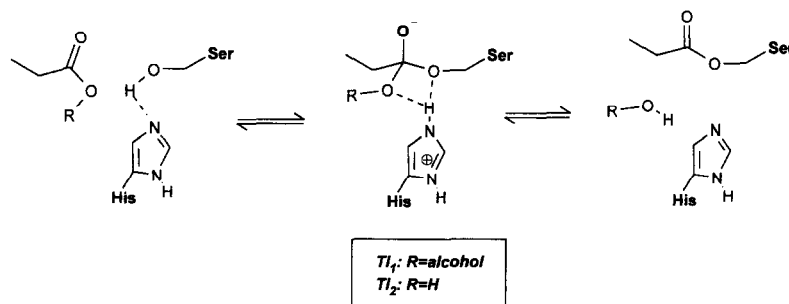


Fig. 1. Proposed tetrahedral intermediates (TI) for the catalytic reactions of esters. (1) Forward reaction TI₁: R = alcohol residue, formation of the acyl enzyme and free alcohol. (2) Reverse reaction TI₂: R = H, nucleophilic attack of water to form the free acid and the regenerated enzyme.

tiopreference as *Candida rugosa* lipase [28,29]. These facts suggests that the lid in any lipase will not have a significant influence on the enantioselectivities in the hydrolysis of esters of chiral alcohols. Therefore we used in this work the structures with open lids.

There exist many different approaches to predict the enantioselectivity. Apart from the improvement of an empirical quantitative model for the hydrolysis of bicyclic secondary alcohols [30] using the CoMFA-method [31], most attempts to model the enantioselectivity have been made by analyzing the conformations of the enantiomers in the binding site of the enzymes and comparing either their structures or their energies. For structural comparison parameters, like numbers of close contacts of the substrate to the enzyme [32] or its relative position within the enzyme [33], are taken from molecular dynamics simulations and used for prediction of enantioselectivities. In energy based analysis, molecular dynamics simulations are used to find minimum energy conformations of diastereomeric complexes [34] or of intermediates [35] which are then used to compare the probabilities of the reaction of the two enantiomeric substrates under consideration.

In the present work, we have first evaluated the minimum energy conformation of the first tetrahedral intermediate, TI_1 , of several *model esters* of secondary and primary alcohols in the binding sites of two different enzymes, namely the lipases from *Candida rugosa* (CRL) [36] and from *Pseudomonas cepacia* (PCL) [37]. These intermediates are considered to be close to the transition states of the reactions and to constitute key structures for the discrimination between the two enantiomeric esters of chiral alcohols. The analyzed *model esters* are esters of simple chiral secondary and primary alcohols which represent the minimum elements of the known empirical rules for enantioselectivity, the substituents at their asymmetric center differing in size and polarity. As in the work of Norin et al. [35], we used the energy differences between the diastereomeric transition states to estimate

enantioselectivities. For this approach to work, the global minimum of the energy for a given model has to be found. Therefore the whole conformational space should be explored in the investigation. Usually, molecular dynamics calculations over a long time span are used [34]. In this work we first used a systematic search to investigate the whole conformational space of the tetrahedral intermediates in the binding sites of the lipases and then a Monte-Carlo type method to sample for minimum conformations within this space. This combination of systematic search and Monte-Carlo minimization method (SsMcm) is very useful for the investigation of constrained systems such as rings or loops in proteins, or small ligands docked in a protein cleft [38] and was already used by us for conformational analysis of triglycerides inside the binding site of CRL [26].

As the energy is just a calculated target function and the energy minimization is a way to find a reasonable three-dimensional arrangement of atoms, very similar structures may show quite different energies. This invariably leads to the phenomenon that the minimization procedure is trapped in a local minimum conformation which differs quite significantly in its energy value with respect to the structurally very close global minimum. To overcome this problem, a short low temperature molecular dynamics calculation was made after the minimization and the resulting structure then minimized again. Using these methods, in most cases a decrease of 2–4 kcal/mol for the different TI_1 -structures was obtained without significant changes in the respective structures (RMS differences of the coordinates were about 0.1 Å).

Some of the predicted enantioselectivities did not match the experimental results on similar substrates. Therefore, for model ester **2** with the largest discrepancy we investigated in a second step the enzyme–substrate complex, without a covalent bond between the serine residue and the carbonyl carbon. Although the relative energies obtained by simulated annealing calculations did not yield better matches, the behavior

in a dynamics simulation of both enantiomers of **2** within the binding site showed some striking differences.

2. Methods

2.1. Molecular modeling equipment

All calculations were performed on Silicon Graphics workstations. The manipulations of molecules, the graphic evaluations, the energy minimizations and the conformational analysis by the Monte-Carlo method were performed using the molecular modeling program-package SYBYL [39].

2.2. Structures of lipases

In this work the X-ray crystal structures of the open lid form of *Candida rugosa* lipase (CRL) [36] (Brookhaven Protein Data Bank entry number 1CRL) and the structure of *Pseudomonas cepacia* lipase (PCL) [37] were used for the conformational analysis of the tetrahedral intermediate in the binding site. All water molecules in the crystal structures were included in the calculations and the hydrogen positions were calculated using the BIOPOLYMER module of SYBYL.

2.3. Force field parameters

For all energy, minimization and dynamics calculations the 'all-atom' AMBER force field [40] in SYBYL [39] was used. Only amino acid residues within an 8 Å distance from the active site serine were allowed to move during the minimization. This way, all residues forming the inner surface of the binding site were allowed to move. The remaining parts of the lipases were constrained to the positions found in the X-ray crystal structure. The minimization was performed by means of the Powell minimizer in SYBYL. In all energy calculations a distance dependent dielectric constant using a

factor of 2 ($\epsilon = 2 \times r$) was used. Non-bonded interactions were truncated at 8 Å.

2.4. Models for the tetrahedral intermediates

All tetrahedral intermediates were modeled by forming a single bond between the reactive carbonyl carbon and the O γ of the serine residue in the active site. The respective active site serine residues are Ser209 in CRL and Ser87 in PCL (see Fig. 2). The carbonyl carbon atom thereby changes to a tetrahedral sp³-hybridized configuration. According to the assumed mechanism [21], the hydrogen atom of the serine is transferred to the imidazole ring of the respective histidine residue. The carbonyl oxygen atom changes to a negatively charged single-bonded oxyanion. The non-standard structural features, such as the bond angles and bond lengths of this tetrahedral intermediate were calculated by the semi-empirical MNDO method in MOPAC [41]. The partial charges of the atoms were calculated, according to the method used for the standard AMBER atom-types [40], from the molecular electrostatic potential using the ESP module in MOPAC. The bond lengths, bond angles and partial charges thus obtained were then used to define a new atom type in the 'all-atom' AMBER force field and to build a serine-substrate complex residue which replaces the corresponding active site residue. For the protonated histidine the existing parameters in the AMBER force field were used. For the *model esters* (1-11) standard AMBER atom types were assigned to the alcohol and acid parts, respectively. The partial charges were also derived from ESP calculations.

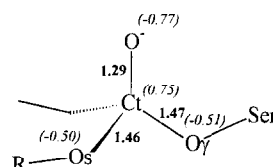


Fig. 2. Used bond lengths (bold) and partial charges (italic) of the tetrahedral intermediate (TI₁).

2.5. Systematic search–Monte-Carlo minimization method (SsMcm)

The Monte-Carlo minimization method [42–44] was successfully applied in the simulation of structural changes of flexible structures. A significant problem with this method lies in the fact, that atomic movements in most directions involve collisions, resulting in large increases in energy. This is especially the case for constrained systems such as rings, loops in proteins or small ligands docked in a protein cleft. This generation of high energy conformations leads to the problem that the overriding factor for the energy minimization becomes the relief of steric strain or satisfaction of defined constraints and therefore long minimization calculations must be used. To overcome this difficulty, we restricted the number of generated conformations allowing the Monte-Carlo minimization to take its 'new' conformations only from a defined set of conformations. In this work the set was generated by a systematic search, carried out over all torsional angles of the serine-bound intermediate complexes and constrained by the binding site of the respective lipase, generating only sterically tolerable conformations. There are amino acid residues within the active sites of the two lipases which could stabilize the negative charge of the oxyanion of TI₁. Thus we could have further reduced the number of conformations to be investigated by predefining such transition states. However, in order to investigate the possible influence of the type of the substrate on the conformation of the serine side chain, the whole conformational space of the serine-bound intermediate complex was analyzed.

The systematic search in SYBYL was carried out by a systematic variation of all selected torsion-angles with increments of 10°. As the atoms are handled like hard spheres, a softness (flexibility) was introduced in the calculation of close contacts by including reductive scaling factors for the van der Waals radii (vdW-interactions), 1–4 van der Waals interactions and

H-bond interactions. For the 1–4 vdW interactions and for the H-bond interactions always the same scaling factors of 0.87 and 0.65, respectively, were used. In order to obtain a statistically reasonable number of conformations (between 10⁴ and 10⁶) different scaling factors for the general vdW-interactions were used in the calculations, varying between 0.90 and 0.80.

In the subsequent Monte-Carlo minimization a random conformation from this set was taken and the structure was minimized for 100 steps. A Boltzman weighted decision at 300 K determined whether the new structure was accepted. The new starting conformation was then generated by selecting randomly at least 2 torsion angles to be changed and then to look in the set for a conformation which differs from the 'current' conformation in these selected torsion angles. All accepted conformations were compared and only unique conformations were saved in a database, giving a set of minimum conformations. The calculations were performed until further calculations did not lead to new conformations with lower energies.

This combination of systematic search and Monte-Carlo Minimization (SsMcm) developed by Purisima and Hogues [38] has been implemented with the SYBYL macro language SPL, using the systematic-search and minimization modules in SYBYL.

2.6. Molecular dynamics

A short low temperature molecular dynamics calculation was carried out on each of the minimum conformations of the SsMcm method and was intended to move the model to a more relaxed structure with a lower energy value, if possible. Therefore in the dynamics simulations the temperature was raised from 0 to 200 K and kept there for 0.1 ps. The temperature was then decreased to 0 K with time steps of 0.05 ps and temperature steps of 50 K. Using higher temperatures and/or longer simulation periods could lead to completely new conformations. The RMS changes in atomic positions during the dynam-

ics simulations ranged between 0.05 and 0.30 Å.

For the simulated annealing and dynamics calculations of the non-bonded enzyme–substrate complex of **2**, the tetrahedral intermediate was changed into a normal carbonyl group, the hydroxyl group of the *active* serine residue protonated and the imidazole ring of the histidine residue transformed in its neutral form. As a starting conformation, the corresponding coordinates of the lowest energy conformation of the intermediate **2** from previous calculations were used and minimized. The simulated annealing simulation had 10 times a heating period of 500 fs to 300 K and a cooling period of 250 fs to 0 K. The resulting conformations after each cooling period were minimized separately. As the simulated annealing calculation gave a migration of the substrate out of the binding site, a dynamics simulation of 15 ps at 300 K was calculated to analyze the migration for both enantiomers.

3. Results and discussion

The *model esters* (see Fig. 3) were chosen in such a way as to represent the principles of the existing rules of predicting which enantiomer reacts faster. In that way **2**, **3**, **6** and **7** represent *model esters* where the substituents differ mostly in size. Models **3** and **7** are included, because of

possible interactions of aromatic substituents. The other models all exhibit a polar group, such as an alcohol or an ether on one side of the asymmetric center of the alcohol residue. The rules presented in the literature are less reliable in the prediction of the preferred enantiomer when there is a polar substituent [8,45]. The lipases of *Candida rugosa* and *Pseudomonas cepacia*, which are widely used in organic chemistry, by far outnumber other enzymes in terms of rules developed for predicting the enantiopreference. Crystal structures for both enzymes have been determined recently [37].

3.1. Comparison of modeling with crystal structure

The analysis of the crystal structures of the inhibitor complexes of CRL with the (*R*)- and (*S*)-menthyl esters of *n*-hexylphosphonochloridate (MPC, PDB entry code 1LPM and 1LPS) [24] show different orientations of the imidazole ring of the histidine residue in the active site (His449) (see Fig. 4a and Table 1). It was also shown [46], that only one orientation of the asymmetric center at the phosphorus atom (S_P configured) was able to bind. In the following, (*R*)- and (*S*)- will be used to discriminate the enantiomeric menthyl residues which are of interest for this investigation. In the (*R*)-MPC-complex the imidazole ring is rotated by around 60° as compared to the (*S*)-isomer and in the

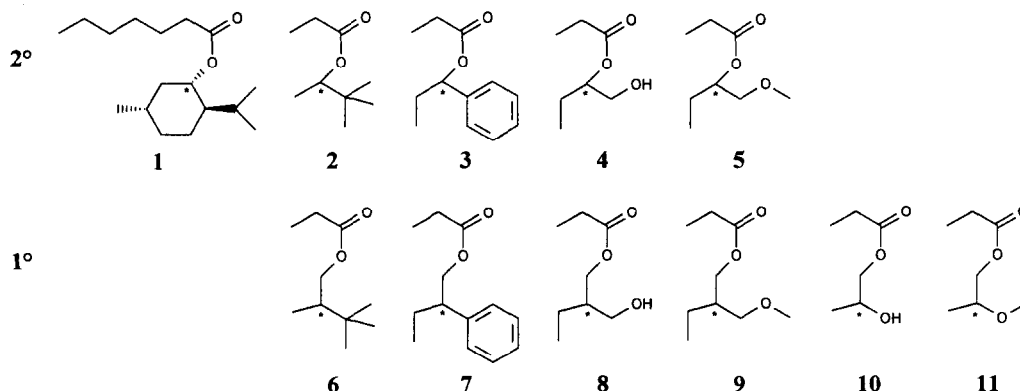


Fig. 3. *Model esters* of chiral secondary (1–5) and primary (6–11) alcohols. The asterisk (*) marks the asymmetric center.

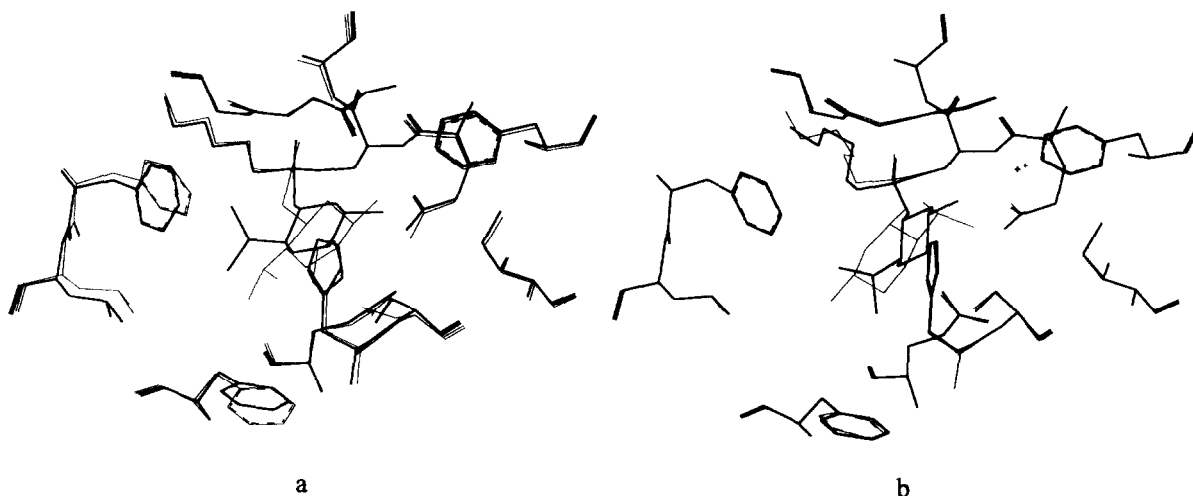


Fig. 4. (a) X-ray crystal structure of (*R*)-MPC (bold) and (*S*)-MPC (thin lines) and (b) minimum energy structure calculated by conformational analysis of (*R*)-1 (bold) and (*S*)-1 (thin lines) in the binding site of CRL. Although the residues in the binding site were allowed to move during minimization, they remained nearly at the same position, only the phenylalanine residue changed slightly. These phenyl rings had also different orientation in the two X-ray crystal structures.

latter structure, no hydrogen bond is formed between the serine alcohol oxygen and *Nε2* of the imidazole ring. This leads to a high energy complex structure. We did energy calculations of the tetrahedral intermediate-enzyme complex 1 using the given coordinates of both crystal structures (1LPM and 1LPS) and replacing the phosphorus atom by the carbonyl carbon of the ester. The minimization with the method described above, resulted in a remarkable energy difference of 18.3 kcal/mol between these diastereomeric complexes. Thereby the difference in the imidazole ring orientation between both diastereomeric complexes decreases to a value of about 18°. The conformational change of the

imidazole ring forced by a large substituent was suggested to be responsible for the discrimination between enantiomers [24]. Superposing both structures, the large and the medium substituent of the asymmetric C atom were pointing towards the same pocket.

An extended conformational search by the SsMcm method of 1 for the (*R*)-diastereomer yielded essentially the same minimum conformation as in the crystal structure, but for the (*S*)-diastereomer a different conformation with a lower energy than the corresponding crystal structure (see Fig. 4b) was found. In this conformation, which exhibits a higher energy of only 3.9 kcal/mol as compared to the (*R*)-di-

Table 1

Torsion angles of the imidazole ring of His445 in the X-ray structure of (*R*) and (*S*)-MPC, compared to this for (*R*) and (*S*)-1 calculated by minimizing the corresponding orientation of the analogue MPC (X-ray + Min) and by extended conformational analysis (SsMcm). The energy differences (ΔE) between both diastereomers of 1 of the whole modeled system (Lip + TI-Ser) and only of the serine-intermediate complex (TI-Ser) are printed

Structure	Torsion angle of imidazole ring of His449 (C α -C β -C γ -N δ 1)		ΔE (<i>R</i> - <i>S</i>) (kcal/mol)	
	(<i>R</i>)	(<i>S</i>)	Lip + TI-Ser	TI-Ser
MPC: X-ray	-123.1	-60.0	—	—
1: X-ray + Min	-93.9	-75.5	-18.26	-21.88
1: SsMcm	-84.5	-85.8	-3.91	-2.61

astereomer, the hydrogen at the asymmetric carbon is oriented towards the same direction as in the other diastereomer and the imidazole ring of His449 has a similar torsion angle. The crystal structures of MPC thus show what we call a **LM**-alignment (large and medium substituent pointing in the same direction for both enantiomers), whereas the calculated structures of **1** show a **H**-alignment (hydrogen pointing in the same direction).

It has to be mentioned that for **1**, as in the MPC-complexes, a hexyl residue was placed at the acid part of the *model ester*, while for all other models (**2** to **11**) a propyl chain was used in the calculations in order to reduce the number of degrees of freedom. Using shorter chain length was considered to be justified by the fact that a detailed analysis of the respective contributions of the various residues of the esters (acid part, alcohol residue etc.) to the overall energies of the substrates revealed that the acyl chain plays only a minor role (0.3 kcal/mol as compared to 1.5 kcal/mol for the alcohol residue).

The results of the calculations for the menthyl ester, although surprising at first sight, do not necessarily represent contradictions to experimental results, since the crystal structures represent low energy conformations of stable complexes, which in the case of the (*S*)-MPC–lipase complex would not necessarily lead directly to hydrolysis. First, the imidazole ring would have to twist again in order to stabilize the alcohol oxygen and to favor by this the breaking of the bond to the carbonyl carbon. Whereas, by modeling the tetrahedral intermediates TI_1 mentioned above, we are analyzing substrates and/or complexes, respectively, which would lead to successful hydrolyses. However, a discrimination of one enantiomer over the other one is guaranteed in both cases.

Apart from the residues on the surface of the binding site, the structure of the lipase is constrained to the position found in the corresponding X-ray structure. Due to limitation of the computer methods and computer resources

larger conformational changes of enzyme domains can not be simulated in an accurate way. For an estimation which part of the enzyme provides the discrimination between the enantiomers, the contributions of the substrate alone to the energy difference of the enantiomers are shown in the tables. However, for the complex **1** the energy differences between the two diastereomeric intermediate–serine complexes and the energy differences between the whole binding site–intermediate complexes are nearly equal. In that sense the energy difference is 2.61 and 3.91 kcal/mol. Using the relationship between free energy difference and enantiomeric ratio [31] this would correspond to an enantiomeric ratio (*E*) of about 80 and >100, respectively, at room temperature. The experimental (*E*)-value for the hydrolysis of menthyl ester by CRL is about 13 [24].

3.2. Oxyanion hole of CRL and PCL

All the conformations revealed a unique orientation of the oxyanion in the binding site of the lipases. In both lipases this negatively charged oxygen is stabilized by two hydrogen bonds, one originating from the neighbouring residue to the serine within the active site. In PCL the protonated amide nitrogens of Leu17 and Gln88 and in CRL those of Ala210 and Gly124 are forming this so called oxyanion hole.

3.3. Secondary alcohol esters

In case of the model of the esters of secondary alcohols, the unique orientation of the tetrahedral intermediate leads also to very unique positions of the alcohol oxygens as well as of the asymmetric carbon. Additionally the hydrogen of the asymmetric carbon atom is always directed to the same side. This restriction is due to the steric features which are part of the catalytic machinery of an esterase. One side is formed by the residues forming the oxyanion hole (see Fig. 5), the other by the imidazole ring

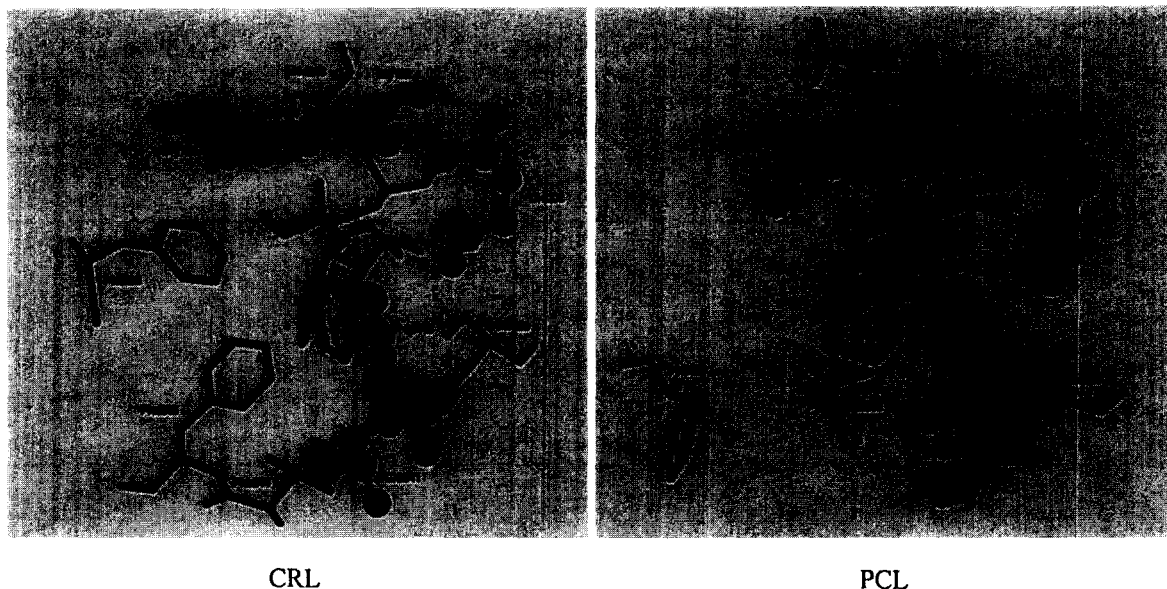


Fig. 5. Minimum energy conformation of the secondary alcohol (*R*)-3 (grey lines) and of the primary alcohol (*R*)-7 (dark lines) in the binding site of CRL and PCL. Thereby, the residues of the three restrictive parts of the binding site, the hydrophilic pocket (light grey), the oxyanion-hole (dark grey) and the residues of the catalytic triad (grey) are shown as ball and stick.

of the histidine (Fig. 5), and the third part is the so-called hydrophilic pocket. The latter is formed in CRL by a glutamic acid and in PCL by a histidine residue, both next to the *active site* serine. Several lipases or esterases exhibit next to their *active site* serine a polar group such as Glu, Asp or His. This structural subunit is supposed [47–49] to trap a water molecule needed for the hydrolysis of the substrate. This water does not influence the conformation of triglycerides within the active site [26] but it does restrict the available space of the pocket in such a way that no big substituent can fit.

These three restrictions can be considered as similar to a three point attachment of any substrate [50], necessary for chiral recognition of a tetrasubstituted carbon. This leads for both investigated lipase structures to a unique orientation of hydrogen (**H**-alignment) and to low energy conformations in which the medium substituent is near the hydrophilic pocket and the large substituent extends towards the solvent or into the hydrophobic pocket. The orientation would correspond to the rule for preferred enantiomer hydrolyses of secondary alcohol by Ka-

zlauskas et al. [3]. The residues of the oxyanion hole restrict the available space in such a way that only a hydrogen can fit. As a matter of fact, only a few enzymatic hydrolyses of esters of tertiary alcohols are known [51]. The imidazole ring of the histidine opposing the oxyanion has to adopt the optimal orientation to form the hydrogen bonds to the oxygens of serine and of the respective alcohol. The energy differences obtained show the same enantiopreferences as the experimental results [7,52–57] for the model 3. For model 2 the calculations showed lower energies for the wrong enantiomer (see Table 2).

For the polar *model esters* with hydroxyl or methoxy groups (4 and 5) the experiments reported in the literature show for most substrates a preference for the enantiomer with the (*R*)-configuration at the asymmetric carbon [58–61]. But for substrates with bigger substituents the preference seems not to be governed by the polar oxygen but by the steric demand of the large substituent [45], leading to a preference for (*S*)-configured esters. The calculations for *model ester 4* (with a hydroxyl group) predicts

Table 2

Torsion angles of the imidazole ring of the *active* His in the calculated minimum energy conformation of the *model ester* of chiral secondary alcohols in the binding site of CRL and PCL. The energy differences (ΔE) between both diastereomers of the whole modeled system (Lip + TI-Ser) and only of the serine-intermediate complex (TI-Ser) are printed. The overlay present which substituent is oriented in the same direction when both enantiomers are superpositioned (L-large substituent, H-hydrogen)

Structure	ΔE (<i>R</i> – <i>S</i>) (kcal/mol)		Torsion ($C\alpha-C\beta-C\gamma-N\delta 1$)		Overlay (alignment of <i>R</i> – <i>S</i>)
	Lip + TI-Ser	TI-Ser	(<i>R</i>)	(<i>S</i>)	
2-crl	0.439	–1.385	–99.8	–94.6	LH
3-crl	–4.867	–7.811	–91.6	–88.6	H
4-crl	2.331	7.037	–100.7	–92.7	H
5-crl	–2.793	–2.568	–99.9	–94.7	H
2-pcl	5.871	4.349	–102.0	–147.5	H
3-pcl	–2.160	–1.531	–113.5	–118.1	H
4-pcl	1.124	3.033	–122.6	–129.0	H
5-pcl	3.817	2.909	–121.6	–124.9	H

preference for the (*S*)-configured ester in both investigated enzymes, whereas for the *model ester* with a methoxy group (**5**), the enantio-preference changed in the CRL binding site (see Table 2). The superposition of the enantiomers for all cases shows H-alignment.

3.4. Primary chiral alcohol esters

The conformations of the *model esters* of apolar chiral primary alcohols like **6** and **7** revealed a similar picture for the carbon next to the alcohol oxygen as in the *model esters* of

chiral secondary alcohols. This carbon has a rather fixed position (within 0.8 Å) and one hydrogen is pointing in the same direction as in the case of the secondary alcohols, whereas the other hydrogen is directed towards the hydrophobic pocket. The asymmetric carbon is situated somehow between the large and medium substituent of the secondary alcohol model. This asymmetric carbon has a greater variety of conformations, but the lowest energy conformations for the energetically favored enantiomer show the large substituent extending towards the hydrophobic large pocket or into the solvent. The

Table 3

Torsion angles of the imidazole ring of the *active* His in the calculated minimum energy conformation of the *model ester* of chiral primary alcohols in the binding site of CRL and PCL. The energy differences (ΔE) between both diastereomers of the whole modeled system (Lip + TI-Ser) and only of the serine-intermediate complex (TI-Ser) are printed. The overlay present which substituent is oriented in the same direction when both enantiomers are superpositioned (L-large substituent, M-medium sized substituent, H-hydrogen)

Structure	ΔE (<i>R</i> – <i>S</i>) (kcal/mol)		Torsion angle of imidazole ring of <i>active</i> histidine ($C\alpha-C\beta-C\gamma-N\delta 1$)		Overlay (alignment of <i>R</i> – <i>S</i>)
	Lip + TI-Ser	TI-Ser	(<i>R</i>)	(<i>S</i>)	
6-crl	0.694	0.971	–96.6	–96.6	L
7-crl	–0.063	–0.313	–100.4	–98.5	H
8-crl	–3.523	–2.892	–96.7	–97.9	H
9-crl	0.319	0.463	–96.5	–96.9	H
10-crl	–0.254	0.001	–94.6	–98.0	M
11-crl	–0.558	–0.386	–100.7	–93.2	L
6-pcl	1.130	0.842	–123.5	–123.2	L
7-pcl	3.552	4.104	–113.3	–131.2	L
8-pcl	–8.226	–9.076	–131.2	–128.3	H
9-pcl	1.664	1.615	–121.5	–120.9	H
10-pcl	4.266	3.305	–117.5	–121.6	M
11-pcl	4.106	1.718	–119.3	–126.3	H

energetically preferred enantiomers show (*S*)-configuration in agreement with the experiment [10,62–64]. This orientation leads to a predominant *L*-alignment (large substituent pointing in the same direction for both enantiomers), in which the large substituents are found roughly in the same area for secondary and primary alcohol models respectively.

In the primary *model esters* with a hydroxyl (**8**, **10**) or methoxy group (**9**, **11**) the alignment of the two enantiomers is different (see Table 3). Most of the calculated polar models show *H*-alignment. For the ester with a hydroxymethyl group (**8**) at the asymmetric carbon, the calculations revealed the (*R*)-configured substrates as preferred enantiomers. This agrees with the limited experimental data reported in the literature for this class of compounds [65]. Surprisingly, the calculated preference changed by replacing the hydroxyl group by a methoxy residue as in **9**. The only reported experimental values were of substrates with an ester group [66,67] instead of the ether group and showed a similar (*R*)-preference with PCL.

By reducing the space between the asymmetric carbon and the hydroxyl group as in **10**, the calculations resulted in (*S*)-preference only for PCL (see Table 3) and remaining the same by adding a methyl group. In case of the CRL a (*R*)-preference resulted in the calculations for both **10** and **11**. The position of the oxygens of the hydroxyl or methoxy groups is similar to the secondary alcohol models **4** and **5**. As with **4** and **5**, experimental results for substrates similar to **10** and **11** [9,67–71] show no unique preference for one configuration, but it seems that the enantioselectivity is determined primarily by the size of the substituents. For polar substrates with small substituents the experimental preferred configuration is (*R*).

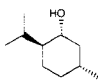
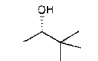
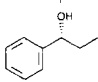
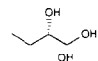
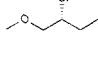
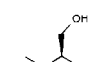
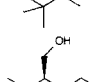
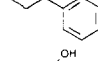
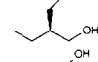
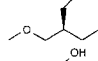
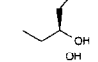
3.5. Comparison with rules and experimental results

The comparison of the computational results with the experimental results and the prediction

by different rules are summarized in Table 4 for CRL and in Table 5 for PCL.

For chiral secondary alcohols in the binding site of CRL the calculations revealed a better agreement with experiments than the prediction

Table 4
Enantioselectivity calculated by conformational analysis, by experiments and predicted by the different rules for the hydrolysis of esters of chiral secondary and primary alcohols by the lipase of *Candida rugosa*. Green values correct, red values incorrect, blue values ambiguous

	Calculations		Experiments ^b		Rules by size ^{c, d}
	Conf	(<i>E</i>) ^a	Conf	(<i>E</i>)	
1		R	>100	R 93 ^e 13 ^k	R
2		S	2	R ^f 30	R
3		R	>100	R ^g -	R
4		S	50	-	(S)
5		R	>100	R ^{h, i} 2-30	(S)
	Calculations		Experiments ^b		Rules (no rules)
	Conf	(<i>E</i>) ^a	Conf	(<i>E</i>)	
6		S	3	-	
7		R	1	-	
8		R	>100	-	
9		S	2	-	
10		R	2	-	
11		R	3	R ^j 30	

Values in parenthesis (**R**) and (**S**) indicate that for model **4** and **5** size derived models are not really applicable.

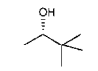
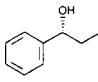
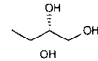
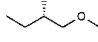
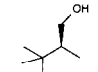
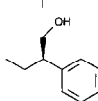
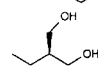
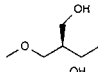
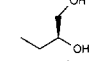
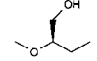
^a (*E*) calculated by the energy difference of the minimum energy conformation of both enantiomers.

^b Experimental value of similar alcohols.

^c Ref. [3]. ^d Ref. [5]. ^e Ref. [72]. ^f Ref. [52]. ^g Ref. [54]. ^h Acetylation with vinyl acetate: Ref. [58]. ⁱ Ref. [59]. ^j Ref. [73]. ^k Ref. [24].

Table 5

Enantiopreference calculated by conformational analysis, by experiments and predicted by the different rules for the hydrolysis of esters of chiral secondary and primary alcohols by *Pseudomonas cepacia* lipase

	Calculations	Experiments ^b		Rules					
		Conf	(<i>E</i>) ^a	Conf	(<i>E</i>)	by size ^{c,d}	models ^{e,f}	by site ^g	
2		S	>100	R ^l	12-20	&		R	
3		R	37	R ^{l,m,n}	50->99		R	R	R
4		S	7	R ^{o,p}	2->100				R
5		S	>100	R ^{o,u}	2				R
				S ^o	42				
	Calculations	Conf	(<i>E</i>) ^a	Experiments ^b	Conf	(<i>E</i>)	Rules	box model ^e	2 rules ^k
				Conf			by size ^{h,i,j}		
6		S	7	S ^{n,q}	3->100	S	S	S	
7		S	>100	S ⁿ	2	S	S	S	
8		R	>100	S ^r	4	(R)	?	(R)	
9		S	16	S ^{k,s}	10-20	(R)	?	(R)	
10		S	>100	-		(S)	?	S	
11		S	>100	R ^{c,j,t}	40-60	(S)	?	S	
				S ^{j,k}	8-42				

Values in parenthesis (**R**) and (**S**) indicate that for model **8**, **9**, **10** and **11** size derived models are not really applicable.

"?" indicates that both enantiomers fit into the box model with no restrictions.

^a (*E*) calculated by the energy difference of the minimum energy conformation of both enantiomers.

^b Experimental value of similar alcohols.

^c Ref. [3]. ^d Ref. [74]. ^e Ref. [6]. ^f Ref. [75]. ^g Ref. [61]. ^h Ref. [8]. ⁱ Ref. [73]. ^j Ref. [9]. ^k Ref. [67]. ^l Esterification with propionic anhydride in benzene: Ref. [53], esterification with vinyl acetate, neat solution: Ref. [76]. ^m Refs. [55,56]. ⁿ Ref. [7]. ^o Refs. [45,59]. ^p Refs. [60,77]. ^q Refs. [62,63]. Kinetic: Ref. [78]. ^r Vinyl acetate: Ref. [65]. ^s Ref. [66]. ^t Refs. [68,71]. ^u Ref. [58].

by the rules. Only **2** gave the wrong enantiomer but with a low enantiomeric ratio (*E*). For chiral primary alcohols experimental values are available only for **11** and CRL exhibits a low enantioselectivity. This was reflected also in the calculations, by low energy differences.

As with CRL, the calculations on **2** in PCL gave the wrong preference. The calculations with **4** gave also a different preference as the experimental results, but these were all resolutions of 1,2 cyclohexanediols, which may have

different steric properties compared with *model ester 4*. For **5** and **11**, no unique preference exists within the experimental data for PCL. The calculations gave in both cases a strong (**S**) preference, whereas the rules are somewhat divergent. On the other hand, the simulation for **5** and **11** for CRL gave the same (**R**) preference as the experimental data.

For *model esters* of primary alcohols only **8** gave a significant different preference as the experimental value. The structure of the pre-

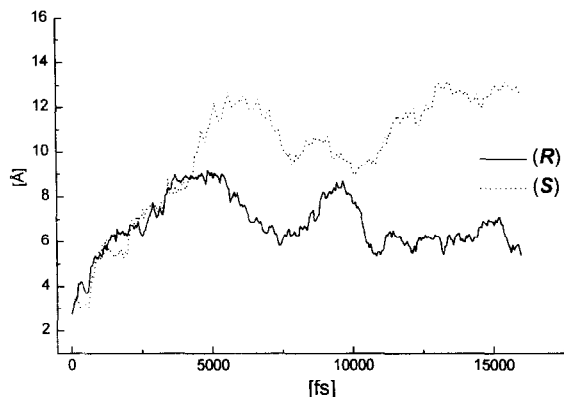


Fig. 6. Distance of the $O_{\gamma}^{\text{Ser209}}$ and the carbonyl C atom in the substrate 2^* of both enantiomers in the binding site of CRL during the dynamics simulations.

ferred (*R*)-**8** revealed that the hydroxyl group was turned back into the hydrophilic pocket. As this pocket is suggested to hold water molecules for the hydrolysis [47–49] this pocket could be filled not only by one water molecule as seen in the crystal structure of CRL, but could contain more molecules, reducing space available for any substrate.

3.6. Investigation of enzyme–substrate complex

As the wrong enantiomer of **2** was the preferred enantiomer in all calculations, we tried

another approach: the difference between the tetrahedral intermediate and the enzyme–non-bonded substrate complex was investigated. Therefore, the tetrahedral intermediate **2** was changed into its free complex, consisting of the ester 2^* and the serine residue. The histidine was thereby changed to its neutral form. As the position of the substrate 2^* had no predefined position, the coordinates of the lowest energy conformation of (*R*)-**2** and (*S*)-**2**, respectively, were transferred to (*R*)- 2^* and (*S*)- 2^* , minimized and followed with a short simulated annealing calculation to find the low energy conformations. In this calculation the simulation with (*S*)- 2^* gave a conformation with a 0.215 kcal/mol lower energy than in the (*R*)- 2^* simulation, still not in agreement with experimental results.

With increasing time, the substrate 2^* moved outside the binding site towards the solvent. A dynamics simulation longer than 15 ps at 300 K showed that 2^* was moving out quite fast and after 2 ps had for both enantiomers already a distance of more than 6 Å from the serine O_{γ} . Fig. 6 shows a plot of the distance between serine O_{γ} and the carbonyl carbon of 2^* versus simulation time. Surprisingly, the two enantiomers were not moving out in the same way.

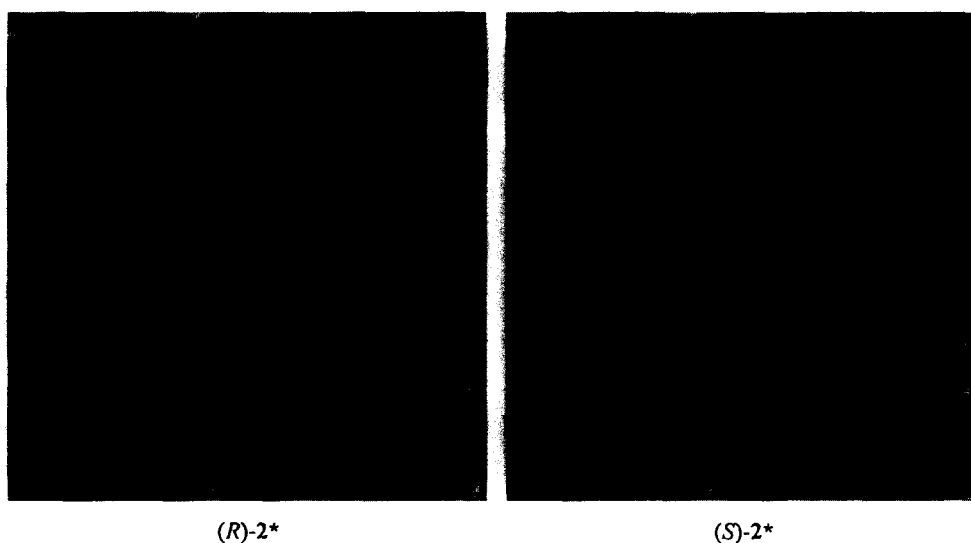


Fig. 7. Trace of the carbonyl C atom position of (*R*)- 2^* and (*S*)- 2^* in the binding site of CRL during dynamic simulations.

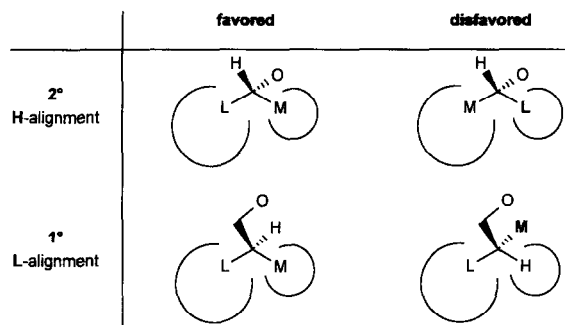


Fig. 8. Orientation of the favored and disfavored enantiomers of chiral secondary and primary alcohol, which have no polar substituents at the asymmetric center.

(*S*)-**2*** moved to a more distant position as seen in Fig. 7. Kinetically this could play a role in the discrimination between the two enantiomers. As long dynamics calculations are extremely computer intensive, no further dynamics simulations on the other substrates have been done yet, but will be the subject of future investigations.

3.7. Alignments

Analyzing the molecular structure of the fast and slow reacting enantiomers constitute the basis for most of the empirical rules for enantioselectivity [3,8]. In this work we describe a similar way by a systematic analysis of the low energy conformations of both enantiomers. Thereby a unique orientation of the favored and disfavored enantiomers in the binding site of both lipases could be detected in the series of

the *model esters* of chiral secondary and primary alcohols with substituents differing mostly in their size (**2**, **3**, **6** and **7**). The orientations of the respective enantiomers changed between the secondary and the primary alcohols (see Fig. 8).

While the secondary alcohols showed **H**-alignment (the hydrogens at the asymmetric center of both enantiomers are directed towards the same site), the primary alcohols exhibit more an **L**-alignment (the large substituents are pointing to the same site). Additionally the large substituents for primary and secondary *model esters* occupy the same pocket, which has been named as the hydrophobic pocket. This pocket is larger than the hydrophilic pocket. The medium substituents for the secondary models are pointing into this hydrophilic pocket, whereas in case of the disfavored enantiomers the large substituents have to fit in this pocket. For primary alcohols, the orientations of the large and medium substituents for the preferred enantiomers are similar to those of the secondary alcohols, leading to opposite configurations at the stereocenter. But for the disfavored enantiomers the medium substituents are partially out of the hydrophilic pocket and more exposed to the solvent.

3.8. Difference between PCL and CRL

Pseudomonas cepacia lipase has a smaller binding site as compared to the lipase from *Candida rugosa*. This results in a greater restric-

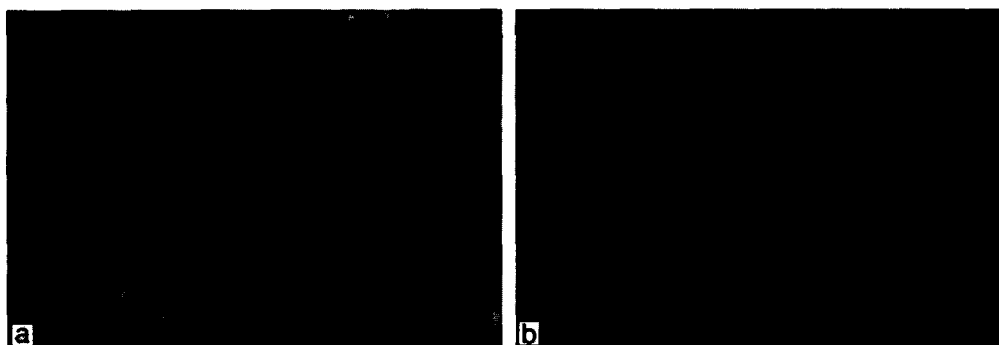


Fig. 9. Topology of the binding site of CRL (a) and PCL (b). Site **A** marks the hydrophilic pocket, **B** the hydrophobic pocket and **C** the acid pocket. Note that in CRL (a) the acid part is found in a tunnel whereas in PCL (b) the acid part is located close to the hydrophobic pocket.

tion for the esters of secondary alcohols, which is also reflected in larger differences between the energies of the respective enantiomers in PCL (see Tables 2 and 3). This smaller binding site could also enhance the influence of the acid part of the esters on the selectivity of the enzyme. Longer acid parts are located close to the hydrophilic pocket and extend towards the solvent along to the large substituents of the preferred enantiomers (see Fig. 9). Large or branched acids will limit the available space within the hydrophobic pocket and can thereby influence the interactions of the alcohol part with the binding site. No influence of the acid part on the binding of the alcohol part can be seen in case of CRL, as this lipase exhibits a separate gorge or tunnel [46] for the acid part of the substrates.

Acknowledgements

We would like to thank Dr. Enrico Purisima for providing the SPL script for the SsMcm method. Thanks also to Dr. Romas Kazlauskas for useful discussions and provision of manuscripts prior to publication. We are also grateful to the Computer Center of the Technical University, Graz for the provision of hardware and computer time. This work was supported by the SFB Biocatalysis.

References

- [1] A. Svendsen, in: P. Wooley and S.B. Petersen (Eds.), *Lipases, their Structure, Biochemistry and Applications* (Cambridge University Press, Cambridge, 1994) pp. 1–48.
- [2] K. Faber, *Biotransformations in Organic Chemistry* (Springer Verlag, Berlin, 1995).
- [3] R.J. Kazlauskas, A.N.E. Weissfloch, A.T. Rappaport and L.A. Cuccia, *J. Org. Chem.* 56 (1991) 2656–2665.
- [4] N.W. Boaz, *J. Org. Chem.* 57 (1992) 4289–4292.
- [5] D. O'Hagan and N.A. Zaidi, *J. Chem. Soc., Perkin Trans. 1*: (1992) 947–949.
- [6] K. Naemura, R. Fukuda, M. Konishi, K. Hirose and Y. Tobe, *J. Chem. Soc., Perkin Trans. 1*: 10 (1994) 1253–1256.
- [7] P. Ferraboschi, S. Casati, S. De Grandi, P. Grisenti and E. Santaniello, *Biocatalysis* 10 (1994) 279–288.
- [8] A.N.E. Weissfloch and R.J. Kazlauskas, *J. Org. Chem.* 60 (1995) 6959–6969.
- [9] G. Carrea, M. De Amici, C. De Micheli, P. Liverani, M. Carnielli and S. Riva, *Tetrahedron* 4 (1993) 1063–1072.
- [10] P.G. Hultin and J.B. Jones, *Tetrahedron Lett.* 33 (1992) 1399–1402.
- [11] Z. Wimmer, *Tetrahedron* 48 (1992) 8431–8436.
- [12] G. Guanti, L. Banfi and E. Narisano, *J. Org. Chem.* 57 (1992) 1540–1554.
- [13] P. Mohr, N. Waespe-Sarcevic and C. Tamm, *Helv. Chim. Acta* 66 (1983) 2501–2511.
- [14] L. Provencher, H. Wynn and J.B. Jones, *Tetrahedron* 4 (1993) 2025–2040.
- [15] L. Provencher and J.B. Jones, *J. Org. Chem.* 59 (1994) 2729–2732.
- [16] E.J. Toone, M.J. Werth and J.B. Jones, *J. Am. Chem. Soc.* 112 (1990) 4946–4952.
- [17] E. Holmberg and K. Hult, *Biocatalysis* 5 (1992).
- [18] S.N. Ahmed, R.J. Kazlauskas, A.H. Morinville, P. Grochulski, J.D. Schrag and M. Cygler, *Biocatalysis* 9 (1994) 209–225.
- [19] A. Warshel, G. Naray-Szabo, F. Sussman and J.-K. Hwang, *Biochemistry* 28 (1989) 3629–3637.
- [20] R.J. Kazlauskas, *Trends Biotechnol.* 12 (1994) 464–472.
- [21] A.A. Kossiakoff and S.A. Spencer, *Biochemistry* 20 (1981) 6462–6474.
- [22] M. Cygler, J.D. Schrag, J.L. Sussman, M. Harel, I. Silman, M.K. Gentry and B.P. Doctor, *Protein Sci.* 2 (1992) 366–382.
- [23] D.L. Ollis, E. Cheah, M. Cygler, B. Dijkstra, F. Frolow, S.M. Franken, M. Harel, S.J. Remington, I. Silman, J. Schrag, J.L. Sussman, K.H.G. Verschuere and A. Goldman, *Protein Eng.* 5 (1992) 197–211.
- [24] M. Cygler, P. Grochulski, R.J. Kazlauskas, J.D. Schrag, F. Bouthillier, B. Rubin, A.N. Serrqia and A.K. Gupta, *J. Am. Chem. Soc.*, 116 (1994) 3180–3186.
- [25] Z.S. Derewenda and Y. Wei, *J. Am. Chem. Soc.* 117 (1995) 2104–2105.
- [26] J. Zuegg, E.O. Purisima and M. Cygler, *in press*.
- [27] R.C. Wade, B.A. Luty, E. Demchuk, J.D. Madura, M.E. Davis, J.M. Briggs and J.A. McCammon, *Stuct. Biol.* 1 (1994) 65–69.
- [28] G. Zandonella, L. Haalck, F. Spener, K. Faber, F. Paltauf and A. Hermetter, *Eur. J. Biochem.* 231 (1995) 50–55.
- [29] M.L.M. Manesse, R.C. Cox, B.C. Koops, M. Verheij, G.H. de Haas, M.R. Egmond, H.T.W.M. v. der Hijden and J. de Vlieg, *Biochemistry* 34 (1995) 6400–6407.
- [30] T. Oberhauser, K. Faber and H. Griengl, *Tetrahedron* 45 (1989) 1679–1682.
- [31] K. Faber, H. Griengl, H. Hönig and J. Zuegg, *Biocatalysis* 9 (1994) 227–239.
- [32] P.A. Fitzpatrick, D. Ringe and A. Klivanov, *Biotechnol. Bioeng.* 40 (1992) 735–742.
- [33] P.R. Ortis de Montellano, J.A. Fruetel, J.R. Collins, D.L. Camper and G.H. Loew, *J. Am. Chem. Soc.* 113 (1991) 3195–3196.
- [34] J. Aerts, *J. Comput. Chem.* 16 (1995) 914–922.
- [35] M. Norin, K. Hult, A. Mattson and T. Norin, *Biocatalysis* 7 (1993) 131–147; J. Uppenberg, N. Ohner, M. Norin, K. Hult, G.J. Kleywegt, S. Patkar, V. Waagen, T. Anthonsen

- and T.A. Jones, *Biochemistry* 34 (1995) 16838–16851; M. Holmquist, F. Haefner, T. Norin and K. Hult, *Protein Sci.* 5 (1996) 83–88.
- [36] P. Grochulski, Y. Li, J.D. Schrag, F. Bouthillier, P. Smith, D. Harrison, B. Rubin and M. Cygler, *J. Biol. Chem.* 268 (1993) 12843–12847.
- [37] J. Schrag, Y. Li and M. Cygler, (1995), personal communication.
- [38] R.O. Purisima and H. Hogues, *J. Cell. Biochem.* 17C (1993) 25.
- [39] SYBYL (Version 6.1), distributed by Tripos Ass. St. Louis, Missouri.
- [40] S.J. Weiner, P.A. Kollman, D.T. Nguyen and D.A. Case, *J. Comput. Chem.* 7 (1986) 230–252.
- [41] MOPAC (Version 6.0), distributed by QCPE, Indiana.
- [42] G. Chang, W.C. Guida and W.C. Still, *J. Am. Chem. Soc.* 111 (1989) 4379–4386.
- [43] N. Go and T. Noguti, *Chem. Scr.* 29a (1989) 151–164.
- [44] Z. Li and H.A. Scheraga, *Proc. Natl. Acad. Sci. USA* 84 (1987) 6611–6615.
- [45] H. Hönl, N. Shi and G. Polanz, *Biocatalysis* 9 (1994) 61–69.
- [46] P. Grochulski, F. Bouthillier, J. Kazlauskas, A.N. Serreqi, J. Schrag, E. Ziomek and M. Cygler, *Biochemistry* 33 (1994) 3494–3500.
- [47] J.S. Schrag, Y. Li, S. Wu and M. Cygler, *Nature* 351 (1992) 761–764.
- [48] J.L. Sussman, M. Harel, F. Frolow, C. Oefner, A. Goldman, L. Toker and I. Silman, *Science* 253 (1991) 872–879.
- [49] M. Norin, F. Haefner and A. Achour, *Protein Sci.* 3 (1994) 1493–1503.
- [50] J.B. Jones, in: J.B. Jones, C.J. Sih and D. Perlman (Eds.), *Applications of Biochemical Systems in Organic Chemistry, Part I* (Wiley, New York, 1976) pp. 1–46.
- [51] J.J. Lalonde, C. Govardhan, N. Khalaf, A.G. Martinez, K. Visuri and A.L. Margolin, *J. Am. Chem. Soc.* 117 (1995) 6845–6852.
- [52] B. Cambou and A.M. Klivanov, *Biotechnol. Bioeng.* 26 (1984) 1449–1454.
- [53] D. Bianchi, P. Cesti and E. Battistel, *J. Org. Chem.* 53 (1988) 5531–5534.
- [54] M. Gruber-Khadjawi, H. Hönl and H. Weber, *Chirality* 4 (1991) 1–7.
- [55] A.L. Gutman, D. Brenner and A. Boltanski, *Tetrahedron: Asymmetry* 4 (1993) 839–844.
- [56] K. Laumen, D. Breitgoff and M.P. Schneider, *J. Chem. Soc. Chem. Commun.* (1988) 1459–1461.
- [57] G. Ottolina, R. Bovara, S. Riva and G. Carrea, *Biotechnol. Lett.* 16 (1994) 923–928.
- [58] Y-F. Wang, J.J. Lalonde, M. Momongan, D.E. Breitbreiter and D.E. Wong, *J. Am. Chem. Soc.* 110 (1988) 7200–7205.
- [59] H. Hönl and P. Scuffer-Wasserthal, *Synthesis* 12 (1990) 1137–1140.
- [60] Z-F. Xie, H. Suemune, I. Naemura and K. Sakai, *Chem. Pharm. Bull.* 35 (1987) 4454–4459.
- [61] Z-F. Xie, I. Nakamura, H. Suemune and K. Sakai, *J. Chem. Soc. Chem. Commun.* (1988) 966–967.
- [62] S. Bart and F. Effenberger, *Tetrahedron* 4 (1993) 823–833.
- [63] D.L. Delinck and A.L. Margolin, *Tetrahedron Lett.* 31 (1990) 6797–6798.
- [64] D.H.G. Crout, D.A. MacManus and P. Critchley, *J. Chem. Soc. Perkin Trans. 1*: (1990) 1865–1868.
- [65] K. Tsuji, Y. Terao and K. Achiwa, *Tetrahedron Lett.* 30 (1989) 6189–6192.
- [66] A. Gaucher, J. Olliver, J. Marguerize, R. Paugam and J. Salaün, *Can. J. Chem.* 72 (1994) 1312–1327.
- [67] Z-F. Xie, H. Suemune and K. Sakai, *Tetrahedron: Asymmetry* 4 (1993) 973–980.
- [68] B. Herradon, *J. Org. Chem.* 59 (1994) 2891–2893.
- [69] Y. Terao, M. Murata, K. Achiwa, T. Nishio, M. Akamitsu and M. Kamimura, *Tetrahedron Lett.* 29 (1988) 5173–5176.
- [70] M. Murata, Y. Terao, K. Achiwa, T. Nishio and T. Seto, *Tetrahedron Lett.* 30 (1989) 2670–2672.
- [71] A. Bosetti, D. Bianchi, P. Cesti and P. Golini, *Biocatalysis* 9 (1994) 71–77.
- [72] G. Langrand, M. Secchi, G. Buono, J. Baratti and C. Trinta-phylides, *Tetrahedron Lett.* 26 (1985) 1857–1860.
- [73] K. Naemura, R. Fukuda, N. Takahashi, M. Konishi, Y. Hirose and Y. Tobe, *Tetrahedron: Asymmetry* 4 (1993) 911–918.
- [74] C.R. Johnson, A. Golebiowski, T.K. McGill and D.H. Steensma, *Tetrahedron Lett.* 32 (1991) 2597–2600.
- [75] K. Burgess and L.D. Jennings, *J. Am. Chem. Soc.* 113 (1991) 6129–6139.
- [76] T. Nishio, M. Kamimura, M. Murata, Y. Terao and K. Achiwa, *J. Biochem. Tokyo* 105 (1989) 510–512.
- [77] Z-F. Xie, H. Suemune and K. Sakai, *J. Chem. Soc. Chem. Commun.* (1987) 838–839.
- [78] M. Indlekofer, M. Reuss, S. Barth and F. Effenberger, *Biocatalysis* 7 (1993) 249–266.